Received: 18 May 2021 | Revised 02 June 2021 | Accepted 05 June 2021

Research Article
Journal of Research and Review in Science, 47-54
Volume 8, June, 2021

DOI:10.36108/jrrslasu/1202.80.0180

ORIGINAL RESEARCH

Climatic Bases and Analyses of Proposed Cloud Attenuation Model for Satellite Links Application

Mustapha Adewusi[1], Oluwafunmilayo Ometan[1], Sayo Akinwumi[2], Temidayo Omotosho[2], Marvel Akinyemi[2], Philips Aizebeokhai[2]

[1]Department of Physics, Faculty of Science, Lagos State University, Nigeria

[2]Department of Physics, College of Science and Technology, Covenant University, PMB 1023, Ota, Ogun State, Nigeria

Correspondence
Mustapha Oladimeji Adewusi, Department of Physics, Faculty of Science, Lagos State University, Nigeria.
Email: mustapha.adewusi@lasu.edu.ng

Funding information
Grant sponsor and grant number: NUC Research Grant (nuc.edu.ng) (NUC1311/1)

Abstract:

Introduction: Established observation showed that larger bandwidth at lower cost is consistently in demand. The demand increases by magnitude of transmission frequency for satellite signal. This is phenomenally accompanied by proportional hydrometeors attenuation. Hence, there is need to evaluate cloud attenuation impact in every climatic region periodically.

Aim: This report is one of the outcomes of experimental communication research carried out at Ota (6.7°N, 3.23°E) tropical station, southwest, Nigeria.

Materials and Methods: The station spectrum analyser measures its received beacons' total attenuation at 12.245 GHz and elevation angle 59.9° to Astra satellites located at 28.2°E. Daily maximum, minimum and mean temperatures; rain amount, wind speed and direction as well as time of occurrence of each of these weather parameters were also measured. Then the radiometric data including acquired radiosonde data were analysed under rainy and non-rainy conditions to obtain cloud attenuation contribution from the total attenuation measured per minute.

Results: The outputs were used to compute the station cumulative distributions for the existing cloud models and for the measured and integrated station's data. Statistical analysis comparing the two cumulative distributions showed a high difference between the measured data and existing models' predicted values.

Conclusion: A cloud attenuation computation algorithm and its simulation program were developed and used to derive a new tropical cloud attenuation model. The results of climatic data and analyses were used to justify the well corroborated new cloud attenuation model.

Keywords: Hydrometeors, Cloud attenuation, Cloud models, Tropical Climate.

All co-authors agreed to have their names listed as authors.

1. INTRODUCTION

In the course of satellite signal's propagation through the atmosphere, it experiences random fluctuations in its wave properties majorly due to attenuation, causing its channel characteristics to change randomly with time. The changes in the channel characteristics results in poor quality of satellite signal reception or totally lost strength in received signal. Clouds are formed by condensation of water vapour on hygroscopic aerosols, which results in formation of cloud condensation nuclei (CCN) when atmosphere is unstable and appropriate lifting mechanism exist. Convection, convergence, frontal and orographic lifts are common lifting mechanisms. Clouds have absorptive, scattering and polarizing effects on electromagnetic signals passing through them [1]. The absorption effect is referred to as cloud attenuation of propagating signal energy by clouds constituent small water droplets. Also, clouds formation is humidity dependent, hence it is time and geographic or location dependent and the tropical lower atmosphere is more often cloudier than in temperate regions [2].

Thus, geomorphological characteristics of each area largely determine the amount of water vapour available there to interact with the hygroscopic aerosols in forming cloud condensation nuclei or cloud droplets. This imply standard satellite services performance may be more difficult to achieve ordinarily in the tropical regions which include more than half of Africa, South America and Australia; about a quarter of North America and half of Asia. Though efforts at solving hydrometeor attenuation effects have yielded reliable and efficient communication media in developed nations; however, lack of necessary local data and needed accurate models have sustained the effects in other nation including most African nations.

The satellite transmission system has the advantage of extremely wide coverage, well above average quality of service, very wide and flexible bandwidth capacity, mobility and low error rate among others [3]. Hence satellite services have graduated into essential category of telecommunication services. A primary signal propagation factor which determines the degree of signal degradation by cloud attenuation is its elevation angle. However, cloud liquid water amount has been established to be proportional to the cloud's attenuation effect on electromagnetic signal that passes through it, such as satellite transmitted signals [4, 5]. The elevation angle determines the length of propagation path and generally the longer the propagation path, the higher the degree of signal degradation [6, 7]. Attenuation or absorption processes at high frequencies is an effect produced by rotational and vibrational transitions in polarized molecules when the electromagnetic signal is incident on the molecules. It has been established that the higher the signal frequency, the more the signal is susceptible to signal fade in the troposphere, though it is less detrimental beyond the troposphere in the upper atmosphere. The processes have quantum nature as the molecular motions occur at specific frequencies [8].

Propagation models have been shown to be necessary to scientifically predict climatic statistics [9, 10]. Attenuation due to clouds can be determined with a great accuracy, using the Rayleigh model which requires assessment of the cloud vertical profile obtained through radiosonde measurements. In this approach, the attenuation estimation depends mainly on the accuracy of the radiosonde measurement [4, 11]. The Rayleigh approach restricts cloud model to non-precipitating clouds for frequency less than 100 GHz, and has been declared accurate for cloud attenuation determination [12, 13, 14].

The design of this study considered measurements and data logging of the station weather parameters, cloud cover (surface and satellite), total hydrometeor attenuation of the earth – space path for the station and its vertical profile.

2. METHODOLOGY

2.1 The Tropical Station Cloud Cover

The research station is tropical Ota (6.7^{o}N, 3.23^{o}E), southwest, Nigeria, whose climatic region mean annual temperature ranges between 26^{o} C and 27^{o} C; and annual rainfall ranges between 2000 mm to 3000 mm [15]. Also, it is common for two or more cloud types to occur simultaneously over the same location but at different heights in the atmosphere, referred to as colocation, this creates need for comparative study of cloud observations from the surface with those from satellite [16]. Hence, cloud parameters measurement method used has two complementary segments namely, satellites clouds observations on one hand and ground visual measurement of clouds at the earth's surface station on the other. Each of these two complementary segments were carried out in this research experiment as designed and are described under the following two subsections. In addition, Weather Link device had been set to measure and log daily maximum, minimum and mean temperatures; rain amount, wind speed and direction as well as time of occurrence of each of these weather parameters, providing the weather state or description during all the measurements in the station.

2.1.1 Cloud Cover Surface Measurements and Data Analysis

In the surface (visual) measurement of the cloud parameters at the station, the sky dome is divided into four quadrants, with respect to the four cardinal directions, for the purpose of determination of the station daily total cloud amounts, cloud types observed; and their respective frequency of occurrence. The station visual observatory being higher than most nearby objects as trees and buildings, offers a clear view of the sky and the clouds. Each assessment view is recorded by a digital camera as a short video, to enable determination of the listed cloud parameters present in the observed cloud layers between their base and maximum vertical distance visible for each of the four sky quadrants, one after the other. The visual cloud cover data are collected twice

daily at fixed times and typical monthly record of the visual data measurement were published [17].

Thus, each daily average cloud amount value is a percentage (%) of the station sky-dome covered by all the cloud types present in the day and the total monthly cloud amount is the average of the station's sky dome covered by all the cloud types present in each day of the month. The average monthly total is computed through the twelve months of each year. Simultaneously, each of the cloud types present were recorded per assessment view daily. Table I shows typical monthly cloud types occurrence data sheet used for monthly calculation of frequency of occurrence of each of the cloud types observed, where the ten cloud types are listed as: cumulus (Cu), stratus (St), stratocumulus (Sc), cumulonimbus (Cb), nimbostratus (Ns), altocumulus (Ac), altostratus (As), cirrocumulus (Cc), cirrostratus (Cs) and cirrus (Ci). In the Table I, the digit 0 represent "absence of a cloud type during an observation" and 1 represent "presence of a cloud type during an observation". The digital digits monthly sum recorded per cloud type per day, for each month were used to compute the frequency of occurrence of each of the cloud types. The monthly cloud amounts, cloud types and their frequencies of occurrence data for 2015 - 2017 were then analysed. The clouds data analyses outcomes are presented under the results and discussion section.

Table I: Typical monthly cloud types occurrence data sheet

	Frequency of Occurrence									
DATE	Cu	St	Sc	Cb	Ns	Ac	As	Cc	Cs	Ci
1-Jul	0	0	1	0	0	1	1	0	0	0
2-Jul										
3-Jul										
4-Jul	0	0	1	0	0	1	1	0	0	0
5-Jul	0	0	1	0	0	1	1	0	0	1
6-Jul	0	0	1	0	0	0	0	0	0	0
7-Jul	1	1	0	0	0	1	1	0	0	0
8-Jul	1	0	1	0	0	1	1	0	0	0
9-Jul										
10-Jul										
11-Jul	1	1	0	0	1	1	1	0	0	0
12-Jul	1	0	0	1	0	1	1	0	0	0
13-Jul	1	1	1	0	1	1	1	0	0	0
14-Jul										
15-Jul	0	0	0	0	0	1	1	0	0	0
16-Jul										
17-Jul										
18-Jul	0	0	1	0	0	1	1	0	0	1
19-Jul	0	0	1	0	0	0	0	0	0	0
20-Jul	1	1	0	0	0	1	1	0	0	0
21-Jul	1	0	1	0	0	1	1	0	0	0
22-Jul										
23-Jul										
24-Jul										
25-Jul	0	0	1	0	0	1	1	0	0	0
26-Jul	0	0	1	0	0	0	0	0	0	0
27-Jul	0	0	1	0	1	0	0	0	0	0
28-Jul	0	1	1	0	1	1	1	0	0	0
29-Jul	1	0	0	0	1	0	0	0	0	0
30-Jul										
31-Jul										
SUM	8	5	13	1	5	14	14	0	0	2
Occurrence (%)	12.90	8.06	20.97	1.61	8.06	22.58	22.58	0.00	0.00	3.23

2.1.2 Satellite Cloud Cover Data and Analysis

The satellite data segment of the station cloud cover determination involves acquisition of satellites observed clouds data over the station. This include the Surface Radiation Budget (SRB) satellite estimated monthly cloud amount (%) for the station between 1998 and 2007; the International Satellite Cloud Climatology Project (ISCCP) satellite estimated monthly mean cloud amount (%) for the station between 1994 and 2008; the Clouds and the Earth's Radiant Energy System (CERES) satellite estimated monthly cloud amount (%), between 2000 and 2014; also CERES_Terra-Aqua-MODIS satellites provided jointly observed station estimated clouds effective heights above the earth surface between 2000 and 2015; the Cloud Aerosol Lidar and Infrared Pathfinder Satellite Observations (CALIPSO) satellite provided estimated monthly clouds amount at high, middle and low clouds categories between 2006 and 2012; CloudSat provided the station estimated monthly clouds amount data between 2006 and 2010 [17].

2.2 Radiometric Measurement and Data Analysis

The station radiometric measurements equipment being used are 9103 spectrum analyser for total hydrometeor attenuation and the Davis weather link climatological device. The spectrum analyser measures every minute the total attenuation on the earth – space path through propagating beacons at 12.245 GHz and elevation angle 59.9o to Astra satellites. Thus, the spectrum analyser measures the total attenuation impact on the beacons propagating to and fro through the earth – space path between the analyser's antenna (outdoor unit) and the Astra satellites. The Davis weather link measures weather parameters such as amount of rainfall, temperature, pressure and humidity, as well as the date and time of their occurrence. The two radiometric devices were connected to a PC for data logging and measurements administration of the station experimental setup. Each of the two devices has a pair of connected outdoor antenna unit and indoor radio unit. Also, the station climatic region radiosonde data of observations for 1953 – 2011 were acquired.

The clouds attenuation contribution data were computed from the measured and logged total attenuation data. The total attenuation (A_T) includes cloud attenuation (A_C), gas attenuation (A_G) and rain attenuation (A_R). It has been established that for transmission frequencies below 45 GHz when scintillation fading and gas attenuation (A_G) may not be very important, Equation (1) is accurate enough for the probable values of A_C, A_G, and A_R to give the total attenuation (A_T) probable value [18, 19, 20].

$$A_T(P) = \sqrt{[(A_G(P))^2 + (A_C(P))^2 + (A_R(P))^2]} \cong \sqrt{[(A_C(P))^2 + (A_R(P))^2]} \quad (1)$$

For the purpose of analysis of the total hydrometeor attenuation data, the tropical station earth –space path has been studied under two conditions - the rainy and non-rainy conditions. The non-rainy condition includes the clear sky and cloudy conditions. The approximation in Equation 1 holds under non-rainy condition, when $(A_R(P))^2 \approx 0$. The climatological device's daily measured and logged data for weather parameters were used in the categorization of the spectrum analyser data into the two study conditions. The persistence of cloud attenuation in all weather conditions necessitate using the rainy and non-rainy weather conditions to evaluate its varying magnitude. The outcomes for the two analysis conditions are presented under results and discussion.

2.3 Development of a Cloud Attenuation Algorithm

The cloud attenuation system equation or algorithm is derived from the consistent geometrical pattern of the station cloud attenuation cumulative distribution for annual spectrum analyser data (SPAD) and the integrated data (ISPAD) shown in Figure 1. The geometry of the integrated cumulative distribution curve describes a resultant constructive interference of some pairs of periodic functions of comparable

amplitudes. Attenuation decreases the amplitude of propagating signal, hence a trigonometric function, specifically cosine function is considered here for its peculiar decreamental nature.

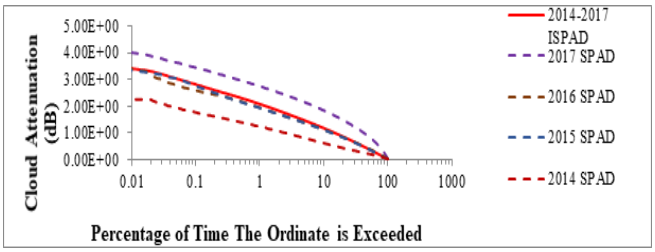

Figure 1: Station annual and ISPAD cloud attenuation cumulative distributions.

The scientific consideration for the possible variables of the system equation focused on the primary cloud parameters namely, the cloud liquid water (WL) and cloud attenuation coefficient (K_L). The two variables vary from one cloud type and layer to another along the propagation path of electromagnetic signals in earth – space path. Analyses result of these observations is mathematically represented by the following general equation [2]:

$$Ac\ (W_L(t,h), K_L(\theta,t,f)) = g(x) = a\cos(x) + b\sin(x) = A\cos(x - \alpha) \quad (2)$$

where $A = (a^2 + b^2)^{1/2}$ and $\alpha = \tan^{-1}(b/a)$ in the range $0 < \alpha < \pi/2$. The independent variables of the cloud attenuation (A_c) are cloud liquid water content (W_L) of each cloud layer having specific attenuation coefficient (K_L) at corresponding temperature (t) and height (h), when propagating radio waves through the cloud layer have angle of elevation (θ) and frequency (f).

The cloud specific attenuation coefficient (K_L) definition is based on the Salonen – Uppala model procedure, adopted by the ITU-R [21]. The K_L definition is based on a mathematical model, using Rayleigh scattering and a double – Debye model for dielectric permitivity Ɛ (f) of water, it is thus defined as:

$$K_L = \frac{0.819\,f}{\varepsilon''(1+\eta^2)}\ (\mathrm{dB/km})/(\mathrm{g/m^3}) \quad (3)$$

The cloud liquid water (W_L) also, is given by the Salonen model (Salonen *et al.*, 1990):

The cloud liquid water (W_L) also, is given by the Salonen model (Salonen *et al.*, 1990):

$$w(t,h) = 3\,w_o.\exp(ct)\left[\frac{h-h_b}{h_r}\right]\ \left(\frac{g}{m^3}\right) \quad (4)$$

Where $h_r = 1500m,\ c = 0.04(^oC^{-1}),\ w_o = 0.17(gm^{-3})$ and such that the liquid and solid water density, w_l and w_i are given by equation (5):

$$w_l(t,h) = w(t,h)\,P_w(t),$$
$$w_i(t,h) = w(t,h)\,[1 - P_w(t)]$$

and

$$P_w(t) = \begin{cases} 1 & 0 < t \\ 1 + \frac{t}{20} & -20 < t < 0^oC \\ 0 & t < -20^oC \end{cases} \quad (5)$$

The resulting algorithm from this analysis is presented under results and discussion.

3. RESULTS AND DISCUSSION

3.1 CLOUD TYPES FREQUENCY OF OCCURRENCE

The ten cloud types were not seen together during any of the observation periods throughout 2015 – 2017. While stratus (St) and stratocumulus (Sc) as well as the altostratus (As) and altocumulus (Ac) were most often than not seen together, cumulus (Cu) occurs with any other cloud types such as stratus (St), stratocumulus (Sc) and nimbostratus (Ns). Stratus (St), stratocumulus (Sc) and nimbostratus (Ns) are sighted alone quite frequently showing their respective high spreading characteristics above 80% in such scenario. The high clouds such as cirrus (Ci), cirrostratus (Cs) and cirrocumulus (Cc) appear much less frequently while cumulonimbus (Cb) rarely occur. Figures 2 and 3 shows the results of the analysis of the cloud type's frequency of occurrence. Data collected from the first to fourth quarter annually in the period show the station characteristics variations of each cloud type's frequency of occurrence in the early dry season relative to late dry season, i.e. first quarter (December to February) relative to late dry season which is second quarter (March to May); similarly early wet season relative to the late wet season i.e. third quarter (June to August) relative to the late wet season which is fourth quarter (September to November).

The two overview graphs (Figures 2 and 3) shows that all the cloud types, except cumulus (Cu) and stratus (St), have higher frequency of occurrence in the wet season (June to November) than in the dry season (December to May). On the average, stratocumulus (Sc) has the highest occurrence at about 23% of the time in the wet season periods and 22% of the time in the dry season periods. This is followed by stratus (St) which is about 17% of the time in the wet season periods and 28% of time in the dry season periods.

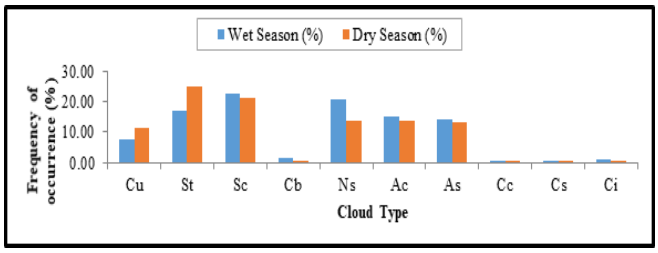

Figure 2: Cloud types frequency of occurrence (%) (2015 - 2016).

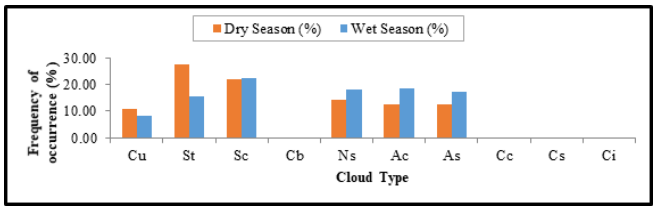

Figure 3: Cloud types frequency of occurrence (%) (2016 – 2017).

Observation further shows that nimbostratus (Ns) occurred about 21% of the time in wet season periods

and about 14% in the dry season periods; while cumulonimbus (Cb) occurrence varies between 0% and about 1.7% of the time in the wet season and about 0% of the time in the dry season periods. Analysis further shows, that the middle clouds altocumulus (Ac) and altostratus (As) often occurred together consistently at about 14% of the time in wet season and 13.5% of the dry season periods. The high clouds (Ci, Cs, and Cc) are largely screened by the low and middle clouds; thus, they are observed at between 0% and 0.8% of wet season periods, and between 0% and about 0.4% of the dry season periods.

3.2 Cloud Amount Distribution

Summarily, analysis of the cloud amounts data indicate that the station cloud amounts exhibit a fairly constant trend in the monthly, quarterly and seasonal averages. Figures 4 and 5 shows that the daily average of the cloud amounts in the wet season varies between 82.3% to 92.7%, while the daily average variation in the dry season ranges between 70.4% to 89.1%; but the daily cloud amount variation through each month is a random distribution.

The monthly averages of the cloud amounts vary from 77.2% in the first month (December) of the dry season to 87.6% at the last month (May) of the season – showing a fairly steady increase between the two ends. The monthly average of the cloud amounts also vary from 89.2% in June - the first month of the wet season to 90.4% in September towards end of the season. The average daily and seasonal cloud amount variations analysis results presented by overview graphs in Figures 4 and 5 shows that the daily cloud amount variation is consistently low in the first and fourth week of every month both in the dry season months and wet season months. This implies high average cloud amount at either ends, while the amplitude of its variation is consistently higher in the second and third week of every month, also both in the dry season months and wet season months. This suggests that relatively heavier rainfall events will most likely occur in the second and third week of every month regardless of the season. This hypothesis seems to explain the relative heights of the station's cloud layers [17]. The range of cloud base heights in the troposphere is lower in the first and last quarter of average year; and higher in the second and third of the average year. This is may be due to higher aerosol – water vapour condensation interaction in the station tropospheric region, where clouds condensation nuclei (CCN) are formed.

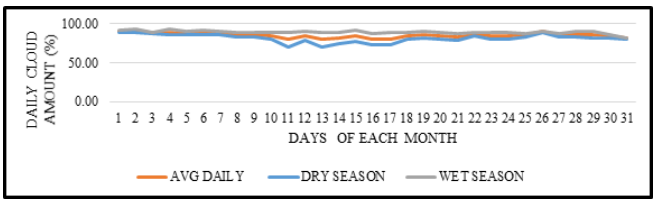

Figure 4: 2015 - 2016 Average daily and seasonal cloud amount.

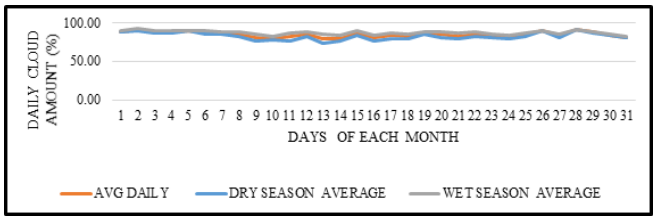

Figure 5: 2016 -2017 Average daily and seasonal cloud amount.

The satellites data were processed and analysed on satellite-by-satellite basis considering one cloud parameter at a time. All the satellites observed and presented clouds amount in percentages of their atmospheric spatial coverages, few estimated clouds liquid water content and only one estimated effective cloud heights of the clouds. Hence, the satellites' cloud data were used to corroborate the stations cloud amount data. Table II shows a comparative summary of the satellites monthly cloud amount which indicates that the satellites overall average cloud amount for the station is 63%, and ranges from 58.3% of the SRB satellite to 80.4% of the CALIPSO satellite. The table also enabled computation of the correlation between the satellite data and ground (visual) data; it is a positive correlation and its value is 0.7885, i.e., 0.8 approximately.

3.3.1 Rainy and Non– Rainy Conditions Radiometric Data Analysis Results

Considering equation (1) and the results of analysis of the daily visual and satellite cloud amounts estimation for this tropical station, the stations' monthly cloud occurrence probability (^{M}Pc) and daily cloud occurrence probability (^{D}Pc) were evaluated using a computation program for probability of cloud occurrence, embedded in the spreadsheets such as shown in Table III. Using the weather device logged data, rainy and non-rainy days of each year were identified. The different daily cloud occurrence probability (^{D}Pc) was used to compute the rainy condition (R) cloud attenuation contribution and the non-rainy condition (nR) cloud attenuation contribution from the measured and logged total attenuation data. Then all the processed cloud attenuation contributions data over 2014 - 2017 were integrated and referred to as integrated spectrum analyser data (ISPAD).

Table II: Satellites and visual monthly clouds amounts statistical summary

	Satellites Monthly Average Cloud Amount						Satelites	Visual Data
	CloudSat	SRB	ISCCP	CERES	CALIPSO	C_T-A-M	Mean	Mean
JAN	15.1606	33.4121	43.6128	49.0370	63.5667	44.6714	41.5768	79.06
FEB	20.2771	42.2097	51.2332	62.7260	76.2187	55.7857	51.4084	79.04
MAR	43.6459	57.9273	68.8875	74.3223	82.6795	65.2335	65.4493	82.07
APR	44.8604	65.7674	74.0642	78.5329	89.8978	68.6588	70.2969	82.13
MAY	49.3148	66.7391	71.2498	76.3202	92.9146	69.3566	70.9825	87.61
JUN	59.0425	70.6840	75.6415	77.7327	87.0072	72.5455	73.7756	89.19
JUL	55.6049	74.8319	82.1054	79.0880	86.8986	75.1494	75.6130	89.99
AUG	61.8760	74.2531	82.7596	75.2827	86.8338	71.1376	75.3571	89.86
SEP	65.8786	75.0585	82.5380	78.1871	88.2813	73.3606	77.2173	90.35
OCT	44.3849	64.1697	71.9371	73.7686	85.5979	64.6955	67.4256	89.60
NOV	30.2021	42.9618	50.2785	53.3699	67.8503	46.8935	48.5927	87.49
DEC	15.2401	32.0395	38.6185	41.4417	56.7292	36.3396	36.7348	77.18
ANNUAL AVG.	42.1240	58.3378	66.0772	68.3174	80.3730	61.9857	62.8692	85.30
S.D. (σ)	17.2197	15.6172	15.1630	12.6934	11.1320	12.3774	13.7330	4.80
Variance	296.5168	243.8963	229.9165	161.1237	123.9222	153.2010	188.5943	23.05
Correlation	0.8558	0.8236	0.7965	0.6834	0.6784	0.7308	0.7882	

Table III: Typical daily probability of cloud occurrence computation program sheet

DEC 2015	Cloud Amount	Rainy Days	Cloudy Days	Clear-sky Days	cRC Filter	cRG Filter	Σ non-Rainy Cloudy Days	Σ non-Rainy Clear-sky Days	MPc	P(Cloud Occurrence) (Pc) DPc (nRD)	Mean DPc	DPc (nR)	DPc (R)
1	83.63	0	1	0	0	0			0.935	0.782	0.737	0.782	0.782
2	85.75	0	1	0	0	0			0.935	0.802		0.802	0.802
3	88.79	0	1	0	0	0			0.935	0.831		0.831	0.831
4	86.15	0	1	0	0	0			0.935	0.806		0.806	0.806
5	87.24	0	1	0	0	0			0.935	0.816		0.816	0.816
6	82.33	0	1	0	0	0			0.935	0.770		0.770	0.770
7	81.75	0	1	0	0	0			0.935	0.765		0.765	0.765
8	79.00	0	1	0	0	0			0.935	0.739		0.739	0.739
9	70.38	0	1	0	0	0			0.935	0.658		0.658	0.658
10	69.11	0	1	0	0	0			0.935	0.646		0.646	0.646
11	62.01	0	0	1	0	0			0.935	0.580		0.580	0.580
12	70.52	0	1	0	0	0			0.935	0.660		0.660	0.660
13	74.49	0	1	0	0	0			0.935	0.697		0.697	0.697
14	87.13	0	1	0	0	0			0.935	0.815		0.815	0.815
15	87.13	0	1	0	0	0			0.935	0.815		0.815	0.815
16	72.38	0	1	0	0	0			0.935	0.677		0.677	0.677
17	74.37	0	1	0	0	0			0.935	0.696		0.696	0.696
18	81.34	0	1	0	0	0			0.935	0.761		0.761	0.761
19	82.01	0	1	0	0	0			0.935	0.767		0.767	0.767
20	78.43	0	1	0	0	0			0.935	0.734		0.734	0.734
21	80.13	0	1	0	0	0			0.935	0.750		0.750	0.750
22	81.63	0	1	0	0	0			0.935	0.764		0.764	0.764
23	72.63	0	1	0	0	0			0.935	0.679		0.679	0.679
24	57.75	0	0	1	0	0			0.935	0.540		0.540	0.540
25	79.63	0	1	0	0	0			0.935	0.745		0.745	0.745
26	83.53	0	1	0	0	0			0.935	0.781		0.781	0.781
27	80.90	0	1	0	0	0			0.935	0.757		0.757	0.757
28	81.26	0	1	0	0	0			0.935	0.760		0.760	0.760
29	82.01	0	1	0	0	0			0.935	0.767		0.767	0.767
30	80.78	0	1	0	0	0			0.935	0.756		0.756	0.756
31	79.32	0	1	0	0	0			0.935	0.742		0.742	0.742
SUMS	78.82	0	29	2	0	0	29	31			0.737		

3.3.2 Analysis of the Cloud Attenuation Cumulative Distributions

The required parameters for evaluation of the attenuation distribution for each of the existing cloud models vary [17]. Most of the cloud models require the signal path length (Lsp) through the cloud layers series (CLS) because the computation of the cloud attenuation is through their respective attenuation coefficient algorithm in dB per kilometer. The extracted radiosonde observations data were used for computation of the predicted cloud attenuation distributions for the station by each of the primary cloud models. Then, the station cloud attenuation cumulative distribution for the 2014 -2017 ISPAD is plotted in the same axes with those of the existing cloud models cumulative distribution curves for comparison as shown in Figure 6. The comparison shows the closest of the existing models to the station ISPAD cloud attenuation cumulative distributions is the ITU-R model, next in closeness is the Liebe model, followed by Slobin model and the Gun and East model.

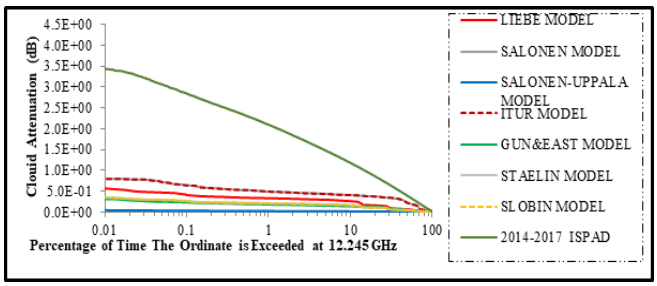

Figure 6: ISPAD and cloud attenuation models cumulative distribution curves.

The comparison shows a wide gap between the 3.40 dB maximum cloud attenuation of the ISPAD cumulative distribution at 0.01% exceedances of station measured data to the 0.7913 dB maximum cloud attenuation predicted by its closest ITU-R model. This empirical result prescribes development of a new model for the tropical region. The result is validated by its agreement with previous results. Reference [4] particularly, reported 2.9 dB maximum cloud attenuation for the 0.01% of time from their cumulative distribution, attributed majorly to 9.5% presence of nimbostratus using data from a similar experimental setup at tropical Penang, when its cloud cover is only 62.4%. Yet another published result state that at time exceedance of 0.01% from their cumulative distribution function, cloud attenuation in the Ka-band can reach up to 4 dB in the tropical region [22].

3.4 The Proposed Cloud Attenuation Model

Cloud attenuation models are experimentally based mathematical algorithm, scientifically designed to predict cloud attenuation impact on propagating electromagnetic signals in earth – space paths from defined location and elevation angle to defined receiver(s) through satellite(s) in uplink or downlink transmission. Having establish that development of a cloud model for the climatic region is necessary, the result of cloud attenuation algorithm development analysis (Equations 2 – 5) is hereby presented as Equation 6.

$$A_c = A_o W_L \cos((0.5K_L) + B) \qquad 0 \le K_L \le \pi \qquad (6)$$

where Ac is the cloud attenuation (dB) in a cloud layer, A_o is the amplitude and B is phase constant of the propagating signal through cloud layer, whose liquid water content is W_L and K_L is its specific attenuation coefficient as defined by the ITU-R. The W_L for station cloud layers were computed from the observation station climatic region radiosonde data. Thus, Equation (6) represents a general cloud attenuation algorithm that can be used to generate a cloud attenuation model for any station's climatic region, provided its two radiometric data are obtainable, i.e., the integrated spectrum analyser data (ISPAD) and the radiosonde data.

To determine the specific equation representing the station cloud attenuation model from the presented cloud attenuation algorithm (Equation 6), a program is

written to run simulation of the algorithm over possible range of the variable constants Ao and B values. The simulations at various values of Ao and B were carried out using $W_L(t, h)$ and $K_L(\theta, t, f)$ data sets generated from the station climatic region's radiosonde data (1953 – 2011). Each simulation corresponds to a pair of possible Ao and B values and generate a set of the station cloud attenuation distribution. Each of the simulation generated station cloud attenuation distribution was statistically analysed using the electronic spreadsheet data analysis tool and cumulative probability distribution function. The output cumulative distribution curve for each generated dataset is compared with the measured climatic region 2014 – 2017 ISPAD cloud attenuation cumulative distribution by placing both of them in the same axes. This is repeated for many sets of (Ao, B) values until a satisfactory matching simulation produce the closest match to the ISPAD cloud attenuation cumulative distribution. The tabulated close simulation cycles parameters indicate that at 12.245 GHz, station data simulation 10.9 produced the closest match to the station integrated cloud attenuation cumulative distribution at 11.5 μm and 1.560796 for A_o and B respectively [17]. Hence, for defined θ range, the station climatic region cloud attenuation model is presented as Equation 7:

$$A_c = 11.5\, W_L \cos((0.5K_L) + 1.560796) \quad (7)$$

Thus, the proposed cloud model was developed analytically and tested statistically through ITU-R procedure, using the extensive radiosonde data and the simulation program to validate the model as shown in Figure 7, with respect to the station ISPAD.

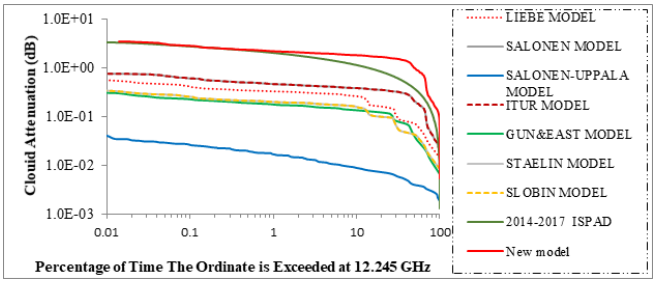

Figure 7: The proposed model and existing cloud models cumulative distributions

Figure 7 shows the new model almost coincide with the station ISPAD in correlation. Though the new model also has similar geometric curve pattern with the existing cloud models in the Ku band frequency considered; however, it revealed the uplink and downlink predictions for cloud attenuation by the primary models largely under estimate the margin for this tropical region.

4. CONCLUSION

The tropical station cloud data revealed that the low cloud types are major contributor to the overall cloud attenuation effects as previously observed in other tropical stations. The common low cloud types over the station climatic region are stratus, stratocumulus and cumulus; while nimbostratus occurs about 20% of the time, cumulonimbus occurs only occasionally. Hence, the southwest Nigeria region weather will most often than not be bright for most part of a year. Thus, the environment is largely conducive for social activities as educational, business and entertainment establishments as well as farming. However, the consistent presence of cloud and their high degree of cloud liquid water amounts present high energy margin needed to successfully communicate satellite electromagnetic signals through the station earth-space path.

The general cloud attenuation algorithm presented in Equation (6) is explicitly quantitative and uniquely based on cosine function; also, it has been constructed to accommodate empirical data. The algorithm can be used to develop the cloud attenuation model for any station climatic region by using the same method described, provided the station's two radiometric data are obtainable, i.e., the spectrum analyser total attenuation data and the radiosonde data. The new model, represented by Equation (7), represents the cloud attenuation profile for tropical southwest Nigeria area having same climatic characteristics as Ota (6.7ºN, 3.23ºE). The profile recommends 4.0 dB margin, for 0.01% of time, needed for satellite signals transmissions to successfully pass-through clouds attenuation effects in the tropical region. These revealed the uplink and downlink predictions for cloud attenuation by the earlier existing models largely under estimate the margin for this tropical region because they were not developed specifically for this climatic region.

ACKNOWLEDGEMENTS

The Covenant University, Ota, Ogun State, Nigeria – the study station, is hereby appreciated for acquisition, installation and provision of the needed measurement instruments used for this research.

COMPETING INTERESTS

Authors have declared that no competing interests exist.

AUTHORS' CONTRIBUTIONS

The corresponding author Mustapha Adewusi, Oluwafunmilayo Ometan and Oluwasayo Akinwumi collected research data jointly under supervision of Prof. Omotosho Temidayo, Prof Marvel Akinyemi and Prof Philips Aizebeokhai.

REFERENCES

1. NASA. The CloudSat Downlink; NASA, 2014, **7**: 1-6.
2. Ippolito, L. J. Satellite communication system engineering. John Willey & Sons, 2008, 1-69.

3. Bruce, R. E. Satellite communication applications. 2nd Edition. Artech House, Inc., Norwood, 2004, 1-65.
4. Mandeep, J. S. and Hassan, S. I. S. Cloud attenuation for satellite applications over equatorial climate. *IEEE AWP Letters,* 2008, **7**: 152-154.
5. Adewusi, O. M., Omotosho, T. V., Akinwunmi, S. A. and Ometan, O. Investigation of low clouds attenuation on earth-space path for some West-Africa stations. *IEEE Xplore*, 2015, 145-148.
6. Zubair, M., Haider, Z., Khan, S. A. and Nasir, J. Atmospheric influences on satellite communications. Przeglad Elektrotechniczny, 2011, **87** (5): 261-264.
7. Ali, M. S., Aduwati, S., Mandeep, J. S. and Ismail, A. Extracted atmospheric impairments on earth-sky signal quality in tropical regions at Ku-band. *J. Atmos. Sol.-Terr. Phys.*, 2013, **104**: 96-105.
8. Rothman, L. S. The HITRAN 2008 molecular spectroscopic database. *J Quant Spectrosc Radiat Transf.*, 2009, **110**(9): 533-572.
9. Willoughby, A. A., Adimula, I. A. and Falaiye, O. A. Effects of rain on microwave and satellite communications in equatorial and tropical regions. *Njphy*, 2005, **17**: 66-71.
10. Hanson, H. and Gray, E. Global precipitation measurement. Core Observatory: GPM Mission Team, NASA, Maryland, 2013, 1-17.
11. Antonio, M., Marina, B., Ermanno, F., Ondrej, F., Frank, S. M., Watson, P. and Wrench, C. Propagation effects due to atmospheric gases and clouds. COST 255, ESA, Netherlands, 2002, **2**: 1-43.
12. Mattioli, V., Basili, F., Bonafora, S., Ciotti, P. and Westwater, E. Analysis and improvements of cloud models for propagation studies. *RDS*, 2009, **44**(2): 1-13.
13. Omotosho, T. V. and Babatunde, E. B. Study of cloud impact on fixed satellite communication link at Ku, Ka and V bands in Nigeria. Austr. *J BAS*, 2010, **4**(8): 3287-3298
14. Eva, R. I., Gustavo A. S., Jose, M. R. and Pedro, G. P. Atmospheric Attenuation in Wireless Communication Systems at Millimeter and THz Frequencies. *IEEE APM*, 2015, **57** (1): 48-61.
15. Frederick, O. A., Garba, M. J. and Adanne I. Secondary Atlas. Macmillan Publishers Limited, Lagos, Nigeria, 2010, 54-55.
16. Warren, S. G., Hahn, C. J. and Eastman, R. M. A survey of changes in cloud cover and cloud types over land from surface observations (1971-96). *J. Clim.*, 2007, **20**: 717-738.
17. Adewusi, O. M., Omotosho T. V., Akinyemi M. L., Akinwumi S. A. and Ometan O. O. Advancement on Cloud attenuation modelling in tropical Ota climatic zone. *EJP*, doi:10.1088/1742-596/1299/1/012049, 2019.
18. Matsudo, T. and Kasarawa Y. Characteristics and prediction methods for the occurrence of SES in available time affected by tropospheric scintillation. *ECJ*, 1991, **74**(8): 89-100.
19. ITU-RP. Propagation data prediction methods required for the design of earth-space telecommunication system. *ITU-RP Recommendation*, 1997, P. 618-5.
20. ITU-R. Attenuation due to Cloud and Fog; *ITU-RP Recommendation*, 2013, P. 840-6.
21. ITU-RP. Attenuation due to clouds and fog. *ITU-RP Recommendation*, 2009, P. 840-4.
22. Yuan, F., Lee, Y. H., Meng, Y. S., Yeo, J. X. and Ong, J. T. Statistical study of cloud attenuation on Ka-band satellite signal in tropical region. *IEEE AWP Letters* 2017, **16**: 2018-2021.